A *Pneumocystis carinii* Group I Intron Ribozyme That Does Not Require 2′ OH Groups on Its 5′ Exon Mimic for Binding to the Catalytic Core[†]

Stephen M. Testa,[‡] Constantine G. Haidaris,[§,∥] Francis Gigliotti,[§,⊥] and Douglas H. Turner*[,‡]

Departments of Chemistry, Microbiology and Immunology, Dental Research, and Pediatrics, University of Rochester, Rochester, New York 14627-0216

Received June 2, 1997; Revised Manuscript Received September 30, 1997[⊗]

ABSTRACT: The recent increase in the population of immunocompromised patients has led to an insurgence of opportunistic human fungal infections. The lack of effective treatments against some of these pathogens makes it important to develop new therapeutic strategies. One such strategy is to target key RNAs with antisense compounds. We report the development of a model system for studying the potential for antisense targeting of group I self-splicing introns in fungal pathogens. The group I intron from the large ribosomal subunit RNA of mouse-derived *Pneumocystis carinii* has been isolated and characterized. This intron self-splices *in vitro*. A catalytically active ribozyme, P-8/4x, has been constructed from this intron to allow measurement of dissociation constants for potential antisense agents. At 37 °C, in 50 mM Hepes (25 mM Na^+), 15 mM $MgCl_2$, and 135 mM KCl at pH 7.5, the exogenous 5′ exon mimic r(AUGACU) binds about 60 000 times more tightly to this ribozyme than to r(GGUCAU), a mimic of its complementary binding site on the ribozyme. This enhanced binding is due to tertiary interactions. This tertiary stabilization is increased by single deoxynucleotide substitutions in the exon mimic at every position except for the internal A, which is essentially unchanged. Thus 2′ OH groups of the 5′ exon mimic do not form stabilizing tertiary interactions with the P-8/4x ribozyme, in contrast to the *Tetrahymena* L-21 *Sca*I ribozyme. Furthermore, at 37 °C, the exogenous 5′ exon mimic d(ATGACT) binds nearly 32 000 times more tightly to the P-8/4x ribozyme than to r(GGUCAU). Therefore, oligonucleotides without 2′ OH groups can exploit tertiary stabilization to bind dramatically more tightly and with more specificity than possible from base pairing. These results suggest a new paradigm for antisense targeting: targeting the tertiary interactions of structural RNAs with short antisense oligonucleotides.

Antisense is a powerful therapeutic approach for targeting RNA (Chrissey, 1991; Baserga & Denhardt, 1992). This approach typically relies on base pairing by a synthetic 15−20 nucleotide antisense agent to its cellular complement, thus disrupting a specific cellular activity. Antisense agents of this length, however, are problematic in terms of synthesis and specificity (Herschlag, 1991; Roberts & Crothers, 1991; Woolf et al., 1992; Wagner et al., 1996). On the basis of studies of oligonucleotide binding to the *Tetrahymena* L-21 *Sca*I group I ribozyme, Bevilacqua and Turner (1991) suggested that shorter oligonucleotides could serve as antisense agents if they were designed to take advantage of tertiary interactions in addition to base pairing. To test this, we have developed a model group I intron system from the opportunistic pathogen *Pneumocystis carinii*. The recent proliferation of this and other fungal pathogens in immunocompromised patients and the need for more effective therapeutics against them makes fungi important targets for pharmacological intervention (Sternberg, 1994).

A group I intron embedded within the large ribosomal RNA of the fungal pathogen *P. carinii* appears to be conserved among different strains of *P. carinii* that infect a wide range of hosts, including rat and human (Liu et al., 1992; Liu & Liebowitz, 1993) as well as ferret and mouse (this work). The absence of group I introns in higher eukaryotes, including humans, suggests therapeutics designed to target group I introns would be highly specific. Since self-splicing of the intron from the ribosomal RNA of *P. carinii* is required for proper ribosomal maturation, and perhaps ribosomal subunit assembly (Nikolcheva & Woodson, 1997), inhibition of the splicing reaction is a potential strategy for pharmacological intervention. In this study, we have isolated a previously undescribed group I intron from the large subunit ribosomal RNA of mouse-derived *P. carinii*. We show that this group I intron self-splices *in vitro*. To allow studies of binding of exogenous 5′ exon mimics to the intron's catalytic core, a ribozyme construct, P-8/4x, was developed. At 37 °C, in 50 mM Hepes (25 mM Na^+), 15 mM $MgCl_2$, and 135 mM KCl at pH 7.5, the 5′ exon mimic r(AUGACU) binds more than 60 000 times more tightly to this ribozyme than it does to its base-pairing complement, r(GGUCAU), a mimic of the ribozyme's internal guide sequence (IGS). This stability enhancement is due to tertiary interactions that form when the 5′ exon mimic·IGS helix docks into the ribozyme's catalytic core. Similar enhanced stabilization is observed with the deoxynucleotide mimics d(AUGACU) and d(ATGACT), which lack 2′ OH groups. This is unexpected, on the basis of results with the *Tetrahymena* ribozyme (Pyle & Cech, 1991; Bevilacqua & Turner, 1991; Pyle et al., 1992; Herschlag et al., 1993; Strobel &

[†] This work was supported by NIH Grant GM22939 to D.H.T., NIH Grant AI23302 to F.G., NIH Grant HL49610 to C.G.H., and NIH postdoctoral fellowship GM17985 to S.M.T.

* Author to whom correspondence should be addressed.
[‡] Department of Chemistry.
[§] Department of Microbiology and Immunology.
[∥] Department of Dental Research.
[⊥] Department of Pediatrics.

[⊗] Abstract published in *Advance ACS Abstracts,* November 15, 1997.

S0006-2960(97)01309-3 CCC: $14.00

Cech, 1993), and indicates that some aspects of the tertiary interactions between the *P. carinii* and *Tetrahymena* ribozymes are dissimilar. These results suggest that oligonucleotides with and without 2′ OH groups can be designed to target RNA by exploiting base-pairing and tertiary interactions. Exploiting tertiary interactions allows short oligonucleotides (on the order of 6 nucleotides) to bind tightly and with much higher specificity to an RNA tertiary-site target than longer oligonucleotides that simply base-pair to their target.

MATERIALS AND METHODS

Oligonucleotide Synthesis and Purification. Oligoribonucleotides and RNA−DNA chimeras were synthesized (Letsinger & Lunsford, 1975; Matteucci & Caruthers, 1980; Sinha et al., 1984; Usman et al., 1987) on an Applied Biosystems solid-phase synthesizer using the manufacturer's suggested protocol for RNA synthesis. Each oligomer was deblocked in 1:3 ethanolic ammonia for 17 h at 55 °C. After the solid support was filtered out, oligomers were incubated in freshly made 1 M TEAHF for 48 h at 55 °C. Thin-layer chromatography was used to separate products from failed sequences using a mobile phase of 1-propanol, concentrated ammonium hydroxide, and distilled water (5.5/3.5/1) on a Baker Si500F TLC plate. After the product was extracted from the silica with water, each oligonucleotide was desalted on a Sep-Pak C18 cartridge (Waters). The acetonitrile used to elute the product was evaporated and the products were stored at −25 °C. The purity of each oligomer was analyzed by HPLC on a Beckman C8 reverse-phase column. The HPLC buffer was 10 mM sodium phosphate (pH 7.0), the mobile phase was methanol, and the gradient was 0−15% methanol over 30 min (1 mL/min). All molecules were at least 95% pure. The concentration of each oligomer was estimated by absorbance at 260 nm using published extinction coefficients (Puglisi & Tinoco, 1989).

Oligodeoxyribonucleotides were synthesized using Applied Biosystem's DNA synthesis protocol and deblocked in concentrated ammonium hydroxide at 60 °C for 1 h. Oligodeoxyribonucleotides shorter than 11 nucleotides were purified by thin-layer chromatography as described above for RNA oligomers. Oligodeoxyribonucleotides longer than 10 nucleotides were synthesized as 5′ trityl-on oligomers. These oligomers were purified from failed sequences and impurities on Poly-Pak reverse-phase cartridges (Glen Research) using the manufacturer's protocol.

r(AUGACU) was 5′ end-labeled by incubating 6.4 pmol of RNA and 27 pmol of [γ-^{32}P]ATP (New England Nuclear) in 50 mM Tris (pH 7.5), 10 mM $MgCl_2$, 5 mM dithiothreitol, 0.1 mM spermidine, and 0.1 mM Na_2EDTA, with 20 units of T4 polynucleotide kinase (Gibco-BRL) in a reaction volume of 20 μL for 30 min at 37 °C. Then 1 μL of glycerol was added and the product was purified on a 20% acrylamide native gel (29:1 acrylamide:bisacrylamide) with 0.25× TBE as the running buffer (1× TBE is 100 mM Tris, 90 mM boric acid, and 1 mM EDTA at pH 8.4). The product was isolated from the gel slice by pulverizing overnight in 500 μL of doubly distilled water with a sterile stir bar (the spin−soak procedure). The gel particulate was spin-filtered out of solution (Isolab, Inc), and the solution was evaporated down to a final oligonucleotide concentration of 8 nM.

P. carinii Group I Intron Isolation and Activity. DNA coding for the *P. carinii* large subunit ribosomal RNA group I intron was isolated from *P. carinii* infected mouse lung and was confirmed to be absent in healthy mouse lung, indicating amplification of *P. carinii* DNA rather than mouse DNA. Similar amplification products were detected in *P. carinii* strains that infect ferret and human lung, indicating that this intron is conserved (data not shown). The group I introns embedded within the large subunit ribosomal RNA (rRNA) plus 75 nucleotides of 5′ exon and 27 nucleotides of 3′ exon were PCR-cloned using primers 4358E d(ACTAAAAGCTTGACGAGGCATTTGGCTACC) and 4359H d(GCGATGAATTCTGCCCAGTGC), which were based upon primers 4358 and 4359 of Liu and Leibowitz (1993). Additional bases were added to primers 4358 and 4359 such that *Eco*RI and *Hin*dIII restriction sites, respectively, were created on the 5′ and 3′ sides of the PCR-amplified product. PCR amplification was conducted in 200 μM of each dNTP, 1 μM each primer, 3 mM $MgCl_2$, 20 mM Tris-HCl (pH 8.4), 50 mM KCl, approximately 2 μg DNA, and 2.5 units of Taq DNA polymerase (Gibco-BRL) in 100 μL total volume. Each of the 35 amplification cycles consisted of 1.5 min at 94 °C, 1.5 min at 65 °C, and 2 min at 72 °C.

The intron from mouse *P. carinii* was further characterized. The amplified product was isolated on a 1.8% agarose gel and subsequently purified using a Sephaglas BandPrep kit (Pharmacia). The product was then reamplified and repurified as above. The group I intron DNA was then unidirectionally ligated into the pGEM-3Zf(+) vector (Promega) downstream of the vector's T7 promoter sequence using the *Eco*RI and the *Hin*dIII restriction sites in the vector and the amplified product, creating the vector P-h (P represents the *Pneumocystis* intron and h that *Hin*dIII linearization of the plasmid produces the correct transcription template) (Figure 2). The vector was then transformed into *Escherichia coli* DH5α competent cells (Gibco-BRL) essentially as outlined (Sambrook et al., 1989) and the vector was purified using a Qiagen Plasmid Mega kit. The inserted fragment was sequenced twice from each end.

The RNA intron precursor was synthesized by T7 RNA polymerase (Davanloo et al., 1984) runoff transcription of the *Hin*dIII-linearized P-h vector. A typical transcription reaction contained 40 mM Tris-HCl (pH 7.4), 1.25 mg/mL BSA, 5 mM spermidine, 5 mM dithiothreitol, 5 mM $MgCl_2$, 1.5 mM each NTP, 1 μg of linearized vector, 4 μL of T7 RNA polymerase (100 units/μL), and 20 pmol of [α-^{32}P]-ATP (New England Nuclear) in 20 μL and was incubated for 1 h at 37 °C. The RNA was purified on a 4% acrylamide/8 M urea gel followed by the spin-soak procedure using 2 mL of polyacrylamide elution buffer [10 mM Tris-HCl (pH 7.4), 1 mM EDTA, and 250 mM NaCl], and then ethanol-precipitated.

Ribozyme Design and Synthesis. A ribozyme construct was synthesized from the *P. carinii* group I intron. This construct lacks the 5′ and 3′ exons so that their binding and activity can be studied with exogenous exon mimics. A T7 RNA polymerase promoter was engineered immediately upstream of the group I intron's P10 IGS (for transcription), and the 3′ end of the ribozyme construct was truncated such that the ribozyme can bind an exogenous 3′ exon mimic (to form element P9.0). The pGEM-9Zf(−) vector (Promega) was used because the vector's natural T7 RNA polymerase promoter could be excised by digesting the vector with restriction enzymes *Sfi*I and *Hin*dIII. Digesting the P-h vector with *Rca*I and *Hin*dIII creates an insert that consists of a truncated 5′ portion of the intron and the entire cloned

3′ exon region. This insert was then ligated into the pGEM-9Zf(−) vector and the resultant gap was filled in with an *Sfi*I−*Rca*I synthetic duplex to create the vector P-8h (-8 represents *8* nucleotides missing from the terminal 5′ end of the transcribed intron). The synthetic duplex contains a 5′ *Sfi*I restriction site, a T7 RNA polymerase promoter 5′ to nucleotide G9 of the intron, and the intron sequence from G9 to T14, which is the cleavage site for *Rca*I. Transcription off the T7 RNA polymerase promoter thus starts at G9 of the intron.

Because there were no natural restriction sites in the 3′ region of the intron, one was created. Nucleotides 337−344, d(ATATTGTG), at the 3′ end of the intron were replaced with d(ATATCTAGA), which creates an *Xba*I restriction site, allowing cleavage after nucleotide T340. The P-8h vector was digested with the restriction enzymes *Hin*dIII and *Nsp*V (which cleaves between nucleotides T323 and C324 of the intron). This fragment was discarded, and a synthetic duplex was ligated in its place. This duplex contains the 3′ half of a *Nsp*V restriction site, the intron sequence from position C324 to T340, an *Xba*I restriction sequence that will produce a cleavage site downstream from nucleotide T340, and a *Hin*dIII restriction sequence for ligating back into the vector. The resultant vector, P-8/4x, when linearized with *Xba*I and transcribed with T7 RNA polymerase produces a ribozyme that consists of nucleotides G9−U340 of the intron (/4 represents the 4 nucleotides missing from the terminal 3′ end of the transcribed intron, and x indicates that *Xba*I linearization of the plasmid produces the correct transcription template). The P-8/4x vector was transformed into *E. coli* DH5α competent cells (Gibco-BRL) and the insert between the T7 promoter and the *Hin*dIII restriction site was sequenced for confirmation.

The ribozyme was synthesized using the same conditions as the full-length intron except that 100 μg of *Xba*I-linearized P-8/4x vector and 500 μL of T7 RNA polymerase (100 units/μL) were used in a reaction volume of 6.9 mL, and a radioactive label was not added to the reaction. The protein was removed by extensive phenol/chloroform extractions followed by ethanol precipitation. The P-8/4x RNA was purified with a Qiagen-tip 500 anion-exchange column following the manufacturer's protocol for purification of runoff transcripts.

Preparation of the *Tetrahymena* L-21 *Sca*I ribozyme was essentially as described above for the P-8/4x ribozyme except that the plasmid pT7L-21 was linearized with the restriction enzyme *Sca*I to form the transcription template (Zaug et al., 1988).

Kinetics. Self-splicing activity was analyzed in buffer H15Mg [50 mM Hepes (25 mM Na^+), 15 mM $MgCl_2$, and 135 mM KCl at pH 7.5] with internally labeled RNA transcribed from the *Hin*dIII-linearized P-h vector. The RNA was typically reannealed by incubating in 1.25× H15Mg buffer at 50 °C for 2 min and then letting it slow cool to 37 °C. Longer 50 °C incubations result in the production of a slowly migrating band that has previously been attributed to a circularization product in other self-splicing introns (Cech et al., 1981; Zaug et al., 1993; Tanner & Cech, 1996). The splicing reaction was started by adding a 37 °C solution of 15 mM pG such that final concentrations in the reaction mixture were 90 nM radiolabeled RNA, 1× H15Mg buffer, and 3 mM pG in a total volume of 30 μL. At selected time intervals, 3-μL aliquots of the reaction mixture were removed and added to an equal volume of stop buffer (0.1× TBE, 10 M urea, and 3 mM EDTA). The aliquots were subsequently run on a 5% acrylamide/8 M urea gel, and then the gel was transferred to chromatography paper (Whatman 3MM CHR) and dried under vacuum for at least 30 min at 60 °C. The bands were quantified on a Molecular Dynamics phosphorimager. Since [pG] ≫ [pre-rRNA], the data were fit to a pseudo-first-order rate equation as described by Bass and Cech (1984) to obtain the observed self-splicing rate constant, k_{obs}.

The P-8/4x ribozyme's ability to catalyze an exon ligation reaction was tested. The ribozyme−substrate complex was prepared in "ribozyme excess" conditions by adding 20 fmol of 5′ end-labeled r(AUGACU) in H15Mg buffer to 4 pmol of P-8/4x ribozyme (preincubated in H15Mg buffer for 8 min at 50 °C) to give a total volume of 15 μL at 37 °C and incubating for 90 min. This is ample time for equilibrium binding to be reached between the two RNAs. The reaction was started by adding 5 μL of a 37 °C solution of a 400 μM stock of r(GUGCUCU) in 1× H15Mg buffer. Aliquots of 2 μL were removed at selected time intervals and added to an equal volume of stop buffer. The aliquots were run on a 20% acrylamide/7 M urea gel to separate reaction products. The bands in the gel were quantified on a Molecular Dynamics phosphorimager. The observed rate constant, k_{obs}, was calculated by fitting the disappearance of radiolabeled r(AUGACU) [to form radiolabeled r(AUGACUCUCU)] vs time to a single-exponential function.

The K_m for r(GUGCUCU) was determined by analyzing the dependence of the single-turnover rate of exon mimic ligation (as above) on the concentration of added r(GUGCUCU). For each single-turnover reaction, at least eight time points were analyzed over 90 min. Between five and eight resultant observed rate constants were used in each of three independent K_m determinations. Each K_m was determined by fitting a plot of the observed reaction rate constant vs concentration using simple Michaelis−Menten kinetics:

$$k_{obs} = (k_{cat}[\text{r(GUGCUCU)}])/([\text{r(GUGCUCU)}] + K_m) \quad (1)$$

where k_{obs} is the observed rate constant, k_{cat} is the maximum catalytic rate constant, [r(GUGCUCU)] is the concentration of substrate, and K_m is the Michaelis constant.

The binding of d(GTGCTCT) and rGrU*d*GrCrUrCrU to P-8/4x was measured by competition with r(GUGCUCU) in the exon ligation reaction. The resultant calculated inhibition constant, K_I, is equivalent to the dissociation constant for binding of the inhibitor to the ribozyme. The K_I of d(GTGCTCT) was measured by adding 60 μM of d(GTGCTCT) to the previously described assay for the determination of the K_m of r(GUGCUCU). For competitive inhibition, the apparent K_m will change upon adding inhibitor according to

$$K_{m(app)} = K_m(1 + ([I]/K_I)) \quad (2)$$

where $K_{m(app)}$ is the apparent K_m of substrate in the presence of inhibitor, K_m is that in the absence of inhibitor, [I] is the inhibitor concentration, and K_I is the inhibition constant (Fersht, 1985).

The K_I of rGrU*d*GrCrUrCrU was measured by adding 60 μM rGrU*d*GrCrUrCrU to an exon ligation reaction containing 20 μM r(GUGCUCU) and the fractional inhibition, *i*, relative to no added inhibitor was used to calculate the K_I:

$$i = (I/K_I)/(1 + (I/K_I) + ([r(GUGCUCU)]/K_m)) \quad (3)$$

The value reported is the average of four independent measurements.

Determination of Binding Constants. The dissociation constant, K_d, of the 5′ exon mimic r(AUGACU) binding to the P-8/4x ribozyme was determined with a direct band-shift electrophoresis assay (Fried & Crothers, 1981; Garner & Revzin, 1981; Pyle et al., 1990, 1994). In this assay, serially diluted concentrations of P-8/4x ribozyme between 1 nM and either 0.15 or 1 μM were reannealed in 6.56 μL total volume containing 3.4% glycerol and 1.14× H15Mg buffer for 8 min at 50 °C. The solution was slow-cooled to 37 °C and 0.94 μL of a stock of ≤8 nM 5′ end-labeled r(AUGACU) at 37 °C was added. After the mixture was incubated at 37 °C for at least 90 min, bound r(AUGACU) was partitioned from that not bound by running 5 μL on a 10% acrylamide native gel. To maintain the integrity of the bound species, the gel and the running buffer were made with H15Mg buffer and were prewarmed to 37 °C before the samples were loaded. It was shown that little to no loss in the percent bound species occurs over the 3−4 min required to load the samples. During this time there is only an insignificant decrease in temperature of the running buffer. The gel was placed on chromatography paper (Whatman 3MM CHR) and dried for no less than 30 min at 60 °C under vacuum. The bands in the gel were quantified on a Molecular Dynamics phosphorimager. The dissociation constant of r(AUGACU) binding to P-8/4x was quantified by fitting the data to the equation (Weeks & Crothers, 1992):

$$\theta = [\text{ribozyme}]_u/([\text{ribozyme}]_u + K_d) \quad (4)$$

where K_d is the dissociation constant of r(AUGACU) and P-8/4x, θ is the fraction of r(AUGACU) bound to the ribozyme, and $[\text{ribozyme}]_u$ is the concentration of unbound ribozyme in the reaction. The value reported is the average of four independent assays.

The K_d of other 5′ exon mimics was determined by competition of each mimic with approximately 1 nM of 5′ end-labeled r(AUGACU) binding to P-8/4x. The assays were conducted essentially as the direct band-shift assay, except that a P-8/4x concentration of 30 nM was used in each assay and the competitor concentration was varied such that the range in each assay flanks the K_d of the competitor in that assay. The ribozyme was reannealed in 5.1 μL of 4.5% glycerol and 1.5× H15Mg buffer, and the binding reaction was initiated by the addition of 2.4 μL of a solution of 3.1 nM 5′ end-labeled r(AUGACU) and various concentrations of competitor. The K_d of each mimic was quantified by fitting the resultant data to a quadratic equation that describes the relationship between the K_d of r(AUGACU) and the K_d of added competitor for binding to P-8/4x (Lin & Riggs, 1972; Weeks & Crothers, 1992). Each K_d value reported is the average of 2−4 independent measurements.

To determine the effects of buffer conditions on the binding of the 5′ exon mimics r(AUGACU) and d(ATGACT) to P-8/4x, competition assays were conducted essentially as above except that T10Mg buffer (50 mM *T*ris, 0.1 mM EDTA, *10* mM *Mg*Cl_2, and 10 mM NaCl at pH 7.5) replaced H15Mg buffer in the binding assay and as the electrophoresis buffer. To determine the effects of buffer conditions on the binding of the corresponding *Tetrahymena* 5′ exon mimics r(CUCUCU) and d(CUCUCU) to the *Tetrahymena* L-21 *Sca*I ribozyme, direct band-shift binding assays were conducted in H15Mg buffer essentially as described above.

Optical Melting Curves. The strength of base pairing between each 5′ exon mimic and an oligonucleotide mimic of the IGS, r(GGUCAU), was analyzed through thermal denaturation experiments at 280 nm on a Gilford 250 UV−vis spectrophotometer equipped with a Gilford 2527 thermoprogrammer. The denaturation process was followed by increasing the temperature of the oligomer solution in H15Mg buffer from 0−60 °C in 60 min and observing the corresponding change in absorbance. The resultant curves were fit using the two-state non-self-complementary model to quantify the thermodynamic parameters of each duplex (Longfellow et al., 1990; McDowell & Turner, 1996). Each molecule was analyzed over a concentration range of approximately 80-fold (typically 8−700 μM), and thermodynamic parameters were also obtained from plots of T_m^{-1} vs log (C_T/4), where T_m is the melting temperature and C_T is the total oligonucleotide concentration (Borer et al., 1974). The agreement of the enthalpy change to within 10% between the two methods is consistent with the two-state assumption.

The oligonucleotide r(GGUCAU) forms a homoduplex that can compete with the formation of the r(GGUCAU)·(5′exon mimic) heteroduplexes. The thermodynamic parameters of the homoduplex were measured as above, except that the two-state self-complementary model was used. The fractions of homoduplex, heteroduplex, and single strands in each sample were then calculated as a function of temperature using the measured thermodynamic parameters (Longfellow et al., 1990). The fraction of homoduplex was always less than 10%, and therefore does not significantly affect the equilibrium and melting curves for the heteroduplex to single strand transition.

Circular Dichroism. Circular dichroism spectra were measured at 3 °C on a Jasco J-710 spectrophotometer from 320−230 nm. The spectrum of each sample was measured five times and averaged.

RESULTS

Large Subunit Ribosomal RNA Group I Intron from P. carinii. The DNA coding for the group I intron and flanking exons from the large subunit ribosomal RNA precursor was isolated from mouse-derived *P. carinii* using PCR primers similar to those used to amplify the corresponding region from rat-derived *P. carinii* (Liu & Leibowitz, 1993). The RNA sequence is shown in Figure 1. The complete homology of the cloned exon sequence and approximately 85% homology of the intron sequence compared with that from rat-derived *P. carinii* (Liu et al., 1992) is a strong indication that the PCR-amplified product is a group I intron embedded within the large subunit ribosomal RNA from mouse-derived *P. carinii*, as expected.

The P-h plasmid (Figure 2) was linearized with the restriction enzyme *Hin*dIII and used as a template for transcription with T7 RNA polymerase. The resultant transcript contains 7 nucleotides from the pGEM-3zf(+) plasmid, followed by 75 nucleotides of 5′ exon, 344 nucleotides of intron, and 27 nucleotides of 3′ exon. The group I intron is able to fold such that it contains all the conserved secondary structure elements normally found in group I introns (Figure 1). The difference in length of the exons was designed to allow separation of reaction products and intermediates on a polyacrylamide electrophoresis gel. Because the RNA was

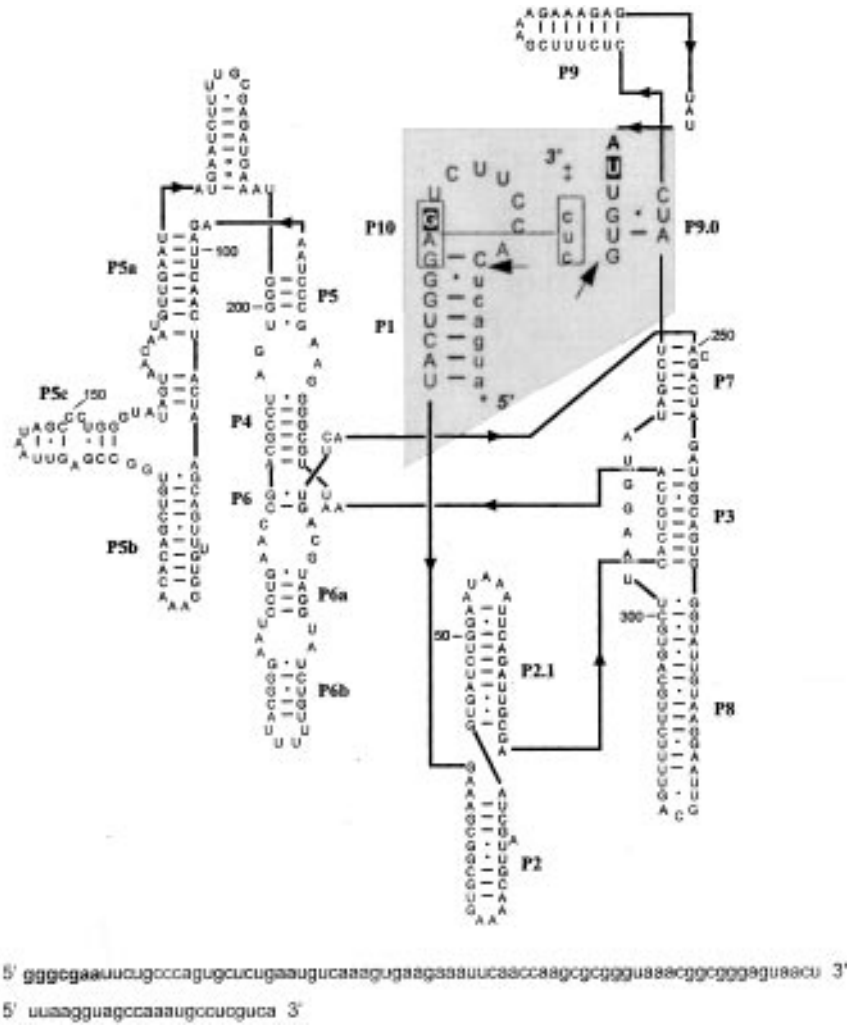

FIGURE 1: Sequence of the flanking exons and group I intron of the *P. carinii* large subunit rRNA and predicted secondary structure. The region containing the 5′ and 3′ exons and their binding sites on the intron is shaded. The arrows point to the 5′ and 3′ splice sites. Exon sequences are in lowercase. The P-8/4x ribozyme consists of bases G9−U340 (G9 and U340 are shown with white lettering and black backgrounds). The conserved helices are labeled as P1−P10. The secondary structure was adapted from the corresponding intron from rat *P. carinii* (Liu & Leibowitz, 1993; Damberger & Gutell, 1994). The boldface nucleotides in the 5′ exon are native to the pGEM-3zf(+) plasmid and are transcribed as part of the ribosomal RNA precursor.

purified by denaturing methods, it was reannealed to produce the functional structure. A 2 min preincubation in H15Mg buffer at 50 °C was sufficient to allow folding of the functional structure, while minimizing circularization products that are visible after a 10 min preincubation.

The conditions used for studying the self-splicing reaction were optimized to maximize the percent of transcripts that self-splice, while maintaining a monovalent ion concentration similar to that found in a typical cell (Harrison & Hoare, 1980). The extent of splicing was maximized at 15 mM $MgCl_2$, 25 mM Na^+, and 135 mM KCl (data not shown), and these conditions were used in subsequent experiments. When the self-splicing reaction is run in Tris buffer, a large amount of an intermediate that lacks the 5′ exon is produced, presumably due to specific hydrolysis at the 5′ splice site. This unwanted side reaction is greatly reduced by running the reaction in Hepes buffer.

The time course of a typical self-splicing reaction (Figure 3A) is shown in Figure 3B. Individual band identities were assigned on the basis of migration properties relative to the unspliced precursor RNA. The conversion of precursor to released intron approaches completion shortly after 20 min. Thus, the group I intron construct from *P. carinii* is able to self-splice *in vitro*. A small amount of intron−3′ exon intermediate is also generated. This intermediate is likely due to either 5′ splice site hydrolysis or release of the 5′ exon after the G-addition reaction and before exon ligation. A small amount of 5′exon−intron intermediate is generated during the 50 °C reannealing protocol. This intermediate is independent of the 37 °C incubation time and is the result of hydrolysis at the 3′ splice site.

The observed rate constant of self-splicing is 0.09 min^{-1} (Figure 3C). This does not include the data point at time zero because a small fraction of precursor splices much faster than most of the precursor. The presence of two rates is seen in other self-splicing group I introns (Barfod & Cech, 1989; Tanner & Cech, 1996). The calculated rate is similar in magnitude to other group I intron self-splicing reactions (Bass & Cech, 1984; Zaug et al., 1993; Weeks & Cech, 1995).

P-8/4x Ribozyme Is Functional. The cloned group I intron DNA was engineered into a ribozyme template by creating an *Xba*I restriction site at the 3′ end of the intron and placing a T7 RNA polymerase promoter immediately upstream of the P10 IGS. Linearizing the resultant plasmid with *Xba*I followed by T7 RNA polymerase transcription creates the P-8/4x ribozyme, which encompasses bases G9−U340 of the intron (Figure 1). This transcript lacks the 5′ and 3′ exons

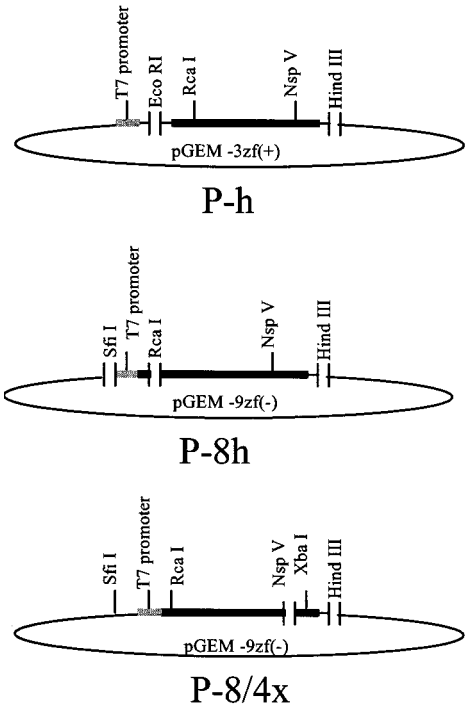

FIGURE 2: Diagrammatic representations of the P-h, P-8h, and P-8/4x plasmids, which were engineered from pGEM plasmids (Promega). Restriction enzyme sites that are boundaries between plasmid and inserts are marked by double vertical hash marks. The T7 RNA polymerase promoter is represented by a gray, bold line. The P-8/4x ribozyme is represented by a black, bold line. The plasmids are not drawn to scale. See text for a description of the plasmid names.

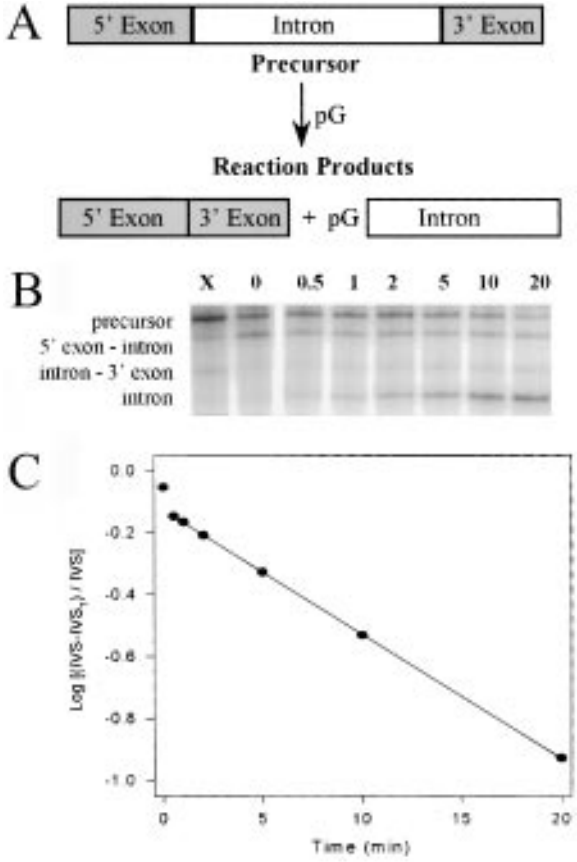

FIGURE 3: Self-splicing reaction in 50 mM Hepes (25 mM Na^+), 15 mM $MgCl_2$, and 135 mM KCl at pH 7.5. (A) Diagrammatic representation of the intron-catalyzed self-splicing reaction. The lengths of the intron and exons are not drawn to scale. (B) The partitioning of the precursor, intermediates, and product of the self-splicing reaction as a function of time (in minutes) on a denaturing polyacrylamide gel. Lane X shows precursor before reannealing, and lane 0, after reannealing and before addition of pG. These two lanes were originally in a different position on the same gel. The intensity of the 5′exon−3′exon product band is very weak due to its relatively small number of radiolabeled adenines and is not shown. (C) The time course of the self-splicing reaction is single-exponential from 0.5 to 20 min. IVS is the fraction of rRNA precursor that can self-splice (determined to be over 0.999 after 80 min), and IVS_T is the fraction of rRNA precursor that is self-spliced at time *T*. The band intensities were normalized for the number of adenines in the RNA of that band. The observed rate constant of self-splicing is the slope of the plot (multiplied by −2.303) of the logarithm of the fraction of unreacted precursor RNA vs time (Bass & Cech, 1984)

and, therefore, allows study of binding and the splicing reaction with exogenous exon mimics. Note that the ribozyme contains the P10 IGS, which allows the 3′ exon mimic to form P10 in addition to P9.0.

The ribozyme's ability to catalyze the exon ligation reaction was examined under single-turnover ribozyme excess conditions. Even though the ribozyme was purified by nondenaturing methods, the ribozyme was preincubated in buffer H15Mg at 50 °C for 8 min to increase the amount of ribozyme folded correctly. There is no observable hydrolysis or degradation of the ribozyme during this preincubation. The time course of a typical exon ligation reaction is shown in Figure 4A. The ribozyme catalyzes ligation, as seen by the increase in reaction product, r(AUGACUCUCU), and decrease of precursor, r(AUGACU). The reaction does not occur in the absence of ribozyme (data not shown). The fact that the ribozyme catalyzes the reaction and is able to bind both the 5′ and 3′ exons is a strong indication that it folds properly under the conditions used in these experiments.

The observed rate constant for ligation, k_{obs}, was quantified from a curve fit of the plot of the percent unreacted precursor vs time (Figure 4B). The dependence of the observed rate constant for ligation on the concentration of 3′ exon mimic, r(GUGCUCU), was fit to a Michaelis−Menten function and gives a maximum rate constant, k_{cat}, of 0.9 ± 0.5 min^{-1} and a K_m of 21 ± 1 μM (see Figure 4C for a representative plot). These results are the averages of three independent assays and the errors are the standard deviations. These results are similar in magnitude to those of a corresponding 3′ exon mimic, r(UCGA), and the *Tetrahymena* L-21 *Sca*I ribozyme using 5 and 50 mM $MgCl_2$ at 15 °C (Bevilacqua et al., 1996).

The G-addition reaction could not be studied in H15Mg buffer because hydrolysis at the 5′ splice site of exogenous 5′ exon mimics, r(AUGACUC) and r(AUGACUCA), is significantly faster than the G-addition reaction (data not shown). This result is surprising because in H15Mg buffer the preincubation and incubation protocols using the full-length group I intron transcript show a very low rate of 5′ splice site hydrolysis. Apparently, the exogenous substrate is bound to the ribozyme such that the 5′ splice site is activated, while the endogenous substrate is not activated. It is likely that sequences in the endogenous 5′ exon play a role in reducing this hyperactivity, which would be deleterious to the cell. The prevalence of hydrolysis is important in that it shows that the ribozyme is binding the 5′ exon mimic and activating the 5′ splice site.

Binding of 3′ Exon Mimics d(GTGCTCT) and rGrUdGrCrUrCrU to the P-8/4x ribozyme. To determine the strength of oligonucleotide binding to the P9.0/P10 site (Figure 1), competitive inhibition of the ribozyme-catalyzed ligation reaction was studied with 3′ exon mimics, d(GTGCTCT)

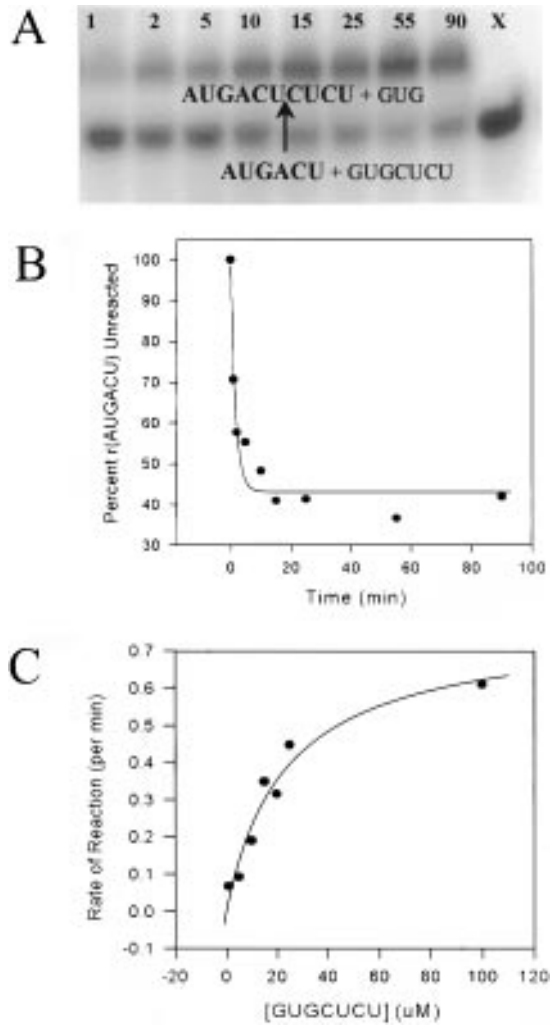

FIGURE 4: Exon ligation reaction catalyzed by 200 nM P-8/4x in 50 mM Hepes (25 mM Na^+), 15 mM $MgCl_2$, and 135 mM KCl, pH 7.5. (A) The partitioning of the substrate, r(AUGACU), and product, r(AUGACUCUCU) of the exon ligation reaction as a function of time (from 1 to 90 min) on a denaturing polyacrylamide gel at 100 μM r(GUGCUCU). Lane X shows the 5′ exon mimic r(AUGACU) incubated with the P-8/4x ribozyme before the addition of the 3′ exon mimic, r(GUGCUCU). (B) Plot and fitted curve of the exon ligation reaction in panel A. (C) Plot and fitted curve of the dependence of the observed rate of exon ligation (k_{obs}) on the concentration of r(GUGCUCU).

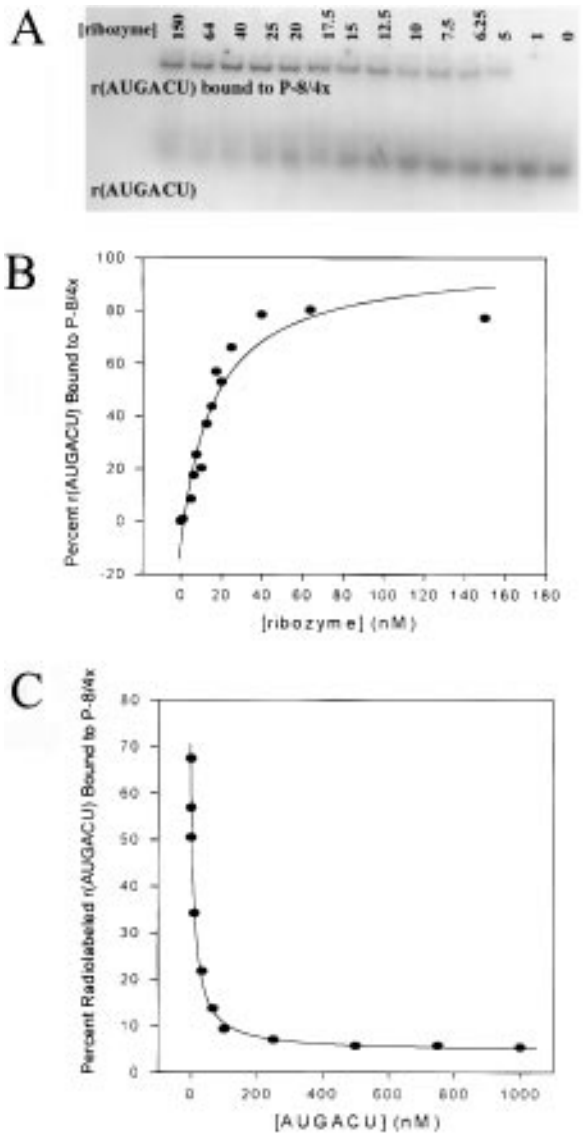

FIGURE 5: Binding of the 5′ exon mimic r(AUGACU) to P-8/4x in 50 mM Hepes (25 mM Na^+), 15 mM $MgCl_2$, and 135 mM KCl at pH 7.5. (A) Partitioning of bound and free r(AUGACU) as a function of P-8/4x concentration (listed in nanomolar above each lane) on a native polyacrylamide gel. (B) Plot and fitted curve of the direct band-shift assay in panel A. Removing the data point where the ribozyme concentration is not in excess over r(AUGACU) does not significantly change the fitted curve. (C) Plot and fitted curve of a competition band-shift assay using r(AUGACU) as a competitor of radiolabeled r(AUGACU) for binding to P-8/4x.

and rGrU*d*GrCrUrCrU. The K_d value for r(GUGCUCU) cannot be directly determined because it is a substrate for ribozyme-catalyzed cleavage. Competitive inhibitors do not change the k_{cat} of a reaction; the inhibitory effect can be overcome by the addition of a high concentration of substrate. The inhibitory effect, therefore, is expressed solely on the apparent K_m of the reaction (see eq 2). The k_{cat} of the splicing reaction with r(GUGCUCU) does not significantly change upon addition of 60 μM d(GTGCTCT) (0.9 min^{-1} without and 0.95 min^{-1} with added inhibitor). The K_m, however, increases from 21 to 33 μM with the addition of inhibitor. This suggests that d(GTGCTCT) is a competitive inhibitor of r(GUGCUCU) for the 3′ exon binding site on the ribozyme. From eq 2, the K_I of d(GTGCTCT) is 107 μM. The K_I of rGrU*d*GrCrUrCrU is estimated from eq 3 to be 40 mM, based upon a 40% reduction in the rate of splicing using 60 μM rGrU*d*GrCrUrCrU, 20 μM r(GUGCUCU), and a K_m of 21 μM. These inhibition constants, K_I, are equivalent to dissociation constants, K_d. On the basis of nearest-neighbor parameters (Sugimoto et al., 1995; Freier et al., 1986), d(GTGCTCT) and r(GUGCUCU) will bind to their RNA complement, r(AGAGCAC), with K_d values of roughly 5 μM and 0.2 μM, respectively, at 37 °C. Thus, oligonucleotides targeted to the P9.0/P10 pairing are unlikely to selectively bind the ribozyme relative to a complementary RNA sequence.

Binding of 5′ Exon Mimic r(AUGACU) to the P-8/4x Ribozyme. The 5′ exon mimic r(AUGACU) binds tight enough to P-8/4x so that the bound complex can be run on a polyacrylamide gel without dissociating. The partitioning on a gel of the radiolabeled exon mimic between that bound to the P-8/4x ribozyme and that not bound (a direct band-shift assay) as a function of P-8/4x concentration is shown in Figure 5A. The average dissociation constant, calculated from three plots of the fraction of 5′ exon mimic bound versus P-8/4x concentration, is 13.9 ± 2.6 nM (see Figure 5B for a representative plot).

As a check on the reliability of the dissociation constant calculated through the direct band-shift method, the K_d of r(AUGACU) binding to the P-8/4x ribozyme was also measured by a competition band-shift assay. The partitioning of the bound and free radiolabeled 5′exon mimic was analyzed using 30 nM P-8/4x ribozyme, 1 nM radiolabeled r(AUGACU), and a variable concentration of added competitor, in this case unlabeled r(AUGACU). The results were quantified with a plot of competitor concentration versus percent radiolabeled 5′ exon mimic bound to P-8/4x (Figure 5C). The average K_d of 5.2 ± 1.4 nM, calculated from three independent assays, is about a third that measured with the direct band-shift method. This difference in values may reflect misfolding of some of the ribozyme and/or subtleties due to the nonequilibrium nature of band-shift assays.

Binding of Deoxy-Substituted 5′ Exon Mimics to the P-8/4x Ribozyme. In order to determine whether the 2′ OH groups of the 5′ exon are involved in tertiary interactions with the P-8/4x catalytic core, binding was measured for 5′ exon mimics containing 1, 5, or 6 deoxynucleotide substitutions. The dissociation constant of each mimic was measured by competition with the radiolabeled 5′ exon mimic r(AUGACU) for binding to the ribozyme (Weeks & Crothers, 1992). The K_d value for r(AUGACU) measured by the direct band-shift assay rather than the value measured by the competition band-shift assay was used in the fits of each resultant competition curve. The measured dissociation constants are shown in Table 1. The mimics that contain single deoxynucleotide substitutions bind roughly as tightly to the ribozyme as r(AUGACU), indicating that no single deoxynucleotide substitution substantially disrupts the base-pairing and tertiary interactions of the 5′ exon mimic. The mimics that contain multiple substitutions bind 10−40-fold less tightly than r(AUGACU) but still much tighter than expected for simple base pairing. Taken together, these results suggest that the 2′ OH groups are not involved in tertiary interactions with the ribozyme.

The tight binding of the 5′ exon mimics containing all deoxynucleotide substitutions was unexpected because the *Tetrahymena* ribozyme binds its corresponding DNA 5′ exon mimic at least 1700 times more weakly than its all-ribonucleotide 5′ exon mimic (Pyle et al., 1990). To determine if the difference in reaction conditions between the two studies accounts for the difference in results, the binding of the 5′ exon mimics d(ATGACT) and r(AUGACU) to P-8/4x was analyzed in the T10Mg buffer of Pyle et al. (1990) by competition band-shift analysis. r(AUGACU) binds with a K_d of 12.4 nM, and d(ATGACT) does not bind tightly enough to quantify by this method. Evidently, some aspects of the tertiary interactions differ in H15Mg and T10Mg buffers for the P-8/4x ribozyme. This large buffer dependence, however, does not extend to the *Tetrahymena* L-21 *Sca*I ribozyme. The *Tetrahymena* ribozyme does not bind its 5′ exon mimic, d(CUCUCU), tightly enough in H15Mg buffer to be quantified. The 5′ exon mimic, r(CUCUCU), however, binds with a K_d of 7 nM in T10Mg buffer (Pyle et al., 1994) and 41 nM in H15Mg buffer (this work). Taken together, these results indicate that some aspects of the tertiary interactions in the two ribozymes are dissimilar.

The *Tetrahymena* ribozyme does not bind the 5′ exon mimic of the P-8/4x ribozyme, r(AUGACU), probably due to an inability of the mimic to base-pair to the *Tetrahymena* ribozyme's IGS (data not shown). This indicates that sequence is an important determinant in the molecular recognition of the 5′ exon mimic, as expected.

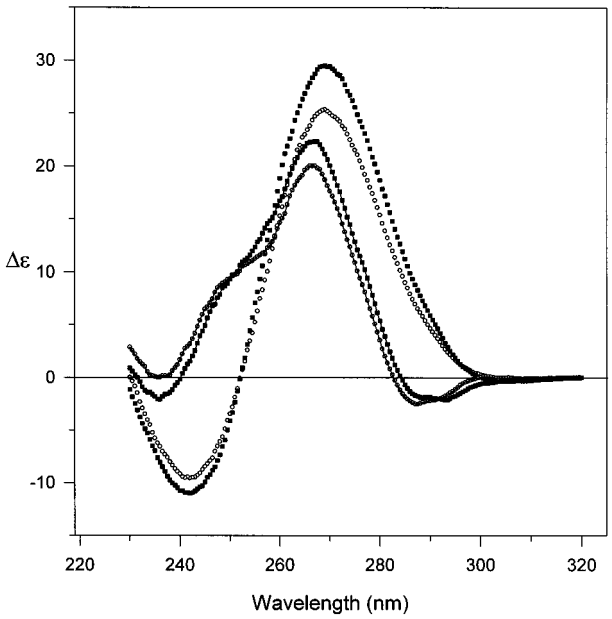

FIGURE 6: CD spectra of 5′ exon mimics r(AUGACU) and d(ATGACT) base-paired with the IGS mimic r(GGUCAU). Spectra were measured in H15Mg buffer (circles) or T10Mg buffer (squares), and the symbols are connected by lines for r(AUGACU). H15Mg buffer consists of 50 mM Hepes (25 mM Na^+), 15 mM $MgCl_2$, and 135 mM KCl at pH 7.5. T10Mg buffer consists of 50 mM Tris, 0.1 mM EDTA, 10 mM $MgCl_2$, and 10 mM NaCl at pH 7.5. All spectra were measured at 3 °C, where over 95% of the oligonucleotides are in the base-paired state, and averaged over 5 scans. The total oligonucleotide concentration was 22.7 μM for each sample.

CD spectra of the duplexes formed by the IGS mimic, r(GGUCAU), with the 5′ exon mimics, r(AUGACU) or d(ATGACT), are not significantly changed by switching from H15Mg to T10Mg buffer (Figure 6). This suggests that the dependence of 5′ exon mimic binding to P-8/4x on buffer conditions is not the result of a buffer-dependent change in global helix conformation of the 5′ exon mimic−IGS base-paired complex. The difference in CD spectra of the RNA duplex and the RNA·DNA hybrid in Figure 6, however, suggests that these duplexes adopt dissimilar global helix geometries, which could affect the stability of tertiary interactions between these duplexes and P-8/4x.

Dissociation Constants of 5′ Exon Mimics Binding to the Oligonucleotide r(GGUCAU). The binding of 5′ exon mimics to the *Tetrahymena* L-21 *Sca*I ribozyme occurs in two major steps. The first step is simple base pairing of the 5′ exon mimic to the IGS of the ribozyme, creating the P1 helix. The second step is docking of the P1 helix into the catalytic core of the ribozyme (Herschlag, 1992; Bevilacqua et al., 1992; Wang et al., 1993). It is likely that binding of 5′ exon mimics to the P-8/4x ribozyme follows the same two-step pathway. To separate the stability increments due to base-pairing and tertiary interactions, the stability due solely to base pairing of each mimic with the IGS oligonucleotide, r(GGUCUA), was measured by thermal denaturation in buffer H15Mg (Table 2). These results show that every 5′ exon mimic that contains a deoxynucleotide forms a less stable helix with r(GGUCAU) than does r(AUGACU).

DISCUSSION

P. carinii Group I Intron. The mouse-derived *P. carinii* group I intron self-splices nearly to completion *in vitro* at a

Table 1: Thermodynamic Parameters for Binding to P-8/4x and r(GGUCAU) in H15Mg Buffer[a]

	binding to P-8/4x		binding to r(GGUCAU)		tertiary stability	
oligonucleotide	K_d[b] (nM)	$-\Delta G°_{37}$[c] (kcal/mol)	K_d[c] (μM)	$-\Delta G°_{37}$[b] (kcal/mol)	$-\Delta\Delta G°_{37}$[d] (kcal/mol)	K_2[e]
rArUrGrArCrU	5.21 ± 1.4	11.75 ± 0.19	318 ± 38	4.96 ± 0.07	6.79 ± 0.20	61 000
dAdTdGdAdCdT	105.3 ± 43	9.90 ± 0.32	3352 ± 167	3.51 ± 0.03	6.39 ± 0.32	31 800
dAdUdGdAdCdU	200 ± 111	9.50 ± 0.50	3462 ± 172	3.49 ± 0.03	6.01 ± 0.50	17 300
dAdTdGdAdC*rU*	61.1 ± 7	10.23 ± 0.075	4072 ± 1208	3.39 ± 0.16	6.84 ± 0.18	66 600
*d*ArUrGrArCrU	3.15 ± 0.35	12.06 ± 0.07	463 ± 47	4.73 ± 0.06	7.33 ± 0.09	147 000
rA*dU*rGrArCrU	6.45 ± 2.85	11.62 ± 0.36	544 ± 37	4.63 ± 0.04	6.99 ± 0.36	84 300
rArU*dG*rArCrU	7.25 ± 3.45	11.55 ± 0.39	1395 ± 118	4.05 ± 0.05	7.50 ± 0.39	192 000
rArUrG*dA*rCrU	15.65 ± 4.05	11.07 ± 0.19	900 ± 45	4.32 ± 0.03	6.75 ± 0.19	57 500
rArUrGrA*dC*rU	4.65 ± 0.2	11.82 ± 0.01	486 ± 76	4.70 ± 0.09	7.12 ± 0.09	104 000
rArUrGrArC*dU*	5.10 ± 0.4	11.76 ± 0.05	544 ± 56	4.63 ± 0.06	7.13 ± 0.08	107 000

[a] H15Mg buffer consists of 50 mM Hepes (25 mM Na^+), 15 mM $MgCl_2$, and 135 mM KCl at pH 7.5. [b] The error is the standard deviation of the measurements. [c] Calculated from $\Delta G°_{37} = RT \ln K_d$, where $R = 0.001987$ kcal mol^{-1} K^{-1} and $T = 310$ K. [d] Calculated from the difference in $\Delta G°_{37}$ from binding to rP3x and r(GGUCAU). This is the free energy increment from tertiary interactions. The error was calculated from the square root of the sum of the squares of each individual error. [e] K_2 is the approximate equilibrium constant for formation of tertiary interactions, calculated by dividing the K_d value for binding to r(GGUCAU) by the K_d for binding to P-8/4x. The K_2 value was calculated using K_d values containing more significant digits than those listed in this table.

Table 2: Thermodynamic Parameters for Binding to r(GGUCAU) in H15Mg Buffer[a]

	$1/T_M$ vs log (C_T/4) parameters				curve fit parameters			
oligonucleotide	$-\Delta G°_{37}$[b] (kcal/mol)	$-\Delta H°$ [b] (kcal/mol)	$-\Delta S°$ [b] (eu)	T_M[c] (°C)	$-\Delta G°_{37}$[b] (kcal/mol)	$-\Delta H°$ [b] (kcal/mol)	$-\Delta S°$ [b] (eu)	T_M[c] (°C)
rArUrGrArCrU	4.96 ± 0.07 (5.6)[d]	44.59 ± 1.8 (50.9)[d]	127.79 ± 6.0 (145.9)[d]	26.4	4.91 ± 0.07	46.41 ± 2.3	133.82 ± 7.6	26.5
dAdTdGdAdCdT	3.51 ± 0.03 (3.1)[d]	55.07 ± 0.6 (40.9)[d]	166.27 ± 2.1 (121.9)[d]	20.9	3.77 ± 0.11	49.82 ± 2.2	148.45 ± 7.4	20.7
dAdTdGdAdC*rU*	3.39 ± 0.16	56.73 ± 2.8	171.97 ± 9.4	20.7	3.51 ± 0.27	52.98 ± 6.0	159.49 ± 20.0	20.3
dAdUdGdAdCdU	3.49 ± 0.03	57.42 ± 0.5	173.88 ± 1.8	21.4	3.78 ± 0.09	51.69 ± 2.2	154.47 ± 7.3	21.3
d*A*rUrGrArCrU	4.73 ± 0.06	45.84 ± 1.5	132.55 ± 5.1	25.3	4.77 ± 0.05	45.16 ± 1.7	130.23 ± 5.6	25.4
rA*dU*rGrArCrU	4.63 ± 0.04	42.31 ± 0.9	121.48 ± 2.9	23.7	4.59 ± 0.20	45.53 ± 5.2	131.98 ± 17.2	24.3
rArU*dG*rArCrU	4.05 ± 0.05	52.18 ± 1.0	155.19 ± 3.5	22.9	4.00 ± 0.10	53.31 ± 2.2	158.97 ± 7.2	23.0
rArUrG*dA*rCrU	4.32 ± 0.03	51.06 ± 0.7	150.69 ± 2.3	24.1	4.42 ± 0.15	49.82 ± 2.8	146.38 ± 9.5	24.4
rArUrGrA*dC*rU	4.70 ± 0.09	47.51 ± 2.1	138.03 ± 7.1	25.5	4.61 ± 0.08	50.93 ± 2.9	149.36 ± 9.3	25.7
rArUrGrArC*dU*	4.63 ± 0.06	46.60 ± 1.2	135.31 ± 4.2	24.9	4.56 ± 0.10	48.69 ± 1.3	142.28 ± 4.3	24.9
rGrGrUrCrArU	3.27 ± 0.09 (3.5)[d]	49.40 ± 1.4 (48.9)[d]	148.72 ± 4.7 (146.5)[d]	22.6	3.55 ± 0.27	45.78 ± 3.0	136.13 ± 10.6	23.3

[a] H15Mg buffer consists of 50 mM Hepes (25 mM Na^+), 15 mM $MgCl_2$, and 135 mM KCl at pH 7.5. [b] The error was calculated as described (SantaLucia et al. 1991a,b; Xia et al., 1997). Significant figures are given beyond error estimates to allow accurate calculation of T_M and other parameters. [c] Calculated for 10^{-4} M oligonucleotide concentration. [d] Predicted from nearest-neighbor parameters (Serra & Turner, 1995; Sugimoto et al., 1995).

rate similar to other self-splicing group I introns (Bass & Cech, 1984; Zaug et al., 1993; Weeks & Cech, 1995). The small percentage that does not self-splice is partially degraded by site-specific hydrolysis, with the 3′ splice site partially hydrolyzed during the 2 min reannealing protocol and the 5′ splice site undergoing hydrolysis mostly during the splicing incubation. That the reaction proceeds on a relatively fast time scale suggests that the group I intron is able to fold correctly in 50 mM Hepes (25 mM Na^+), 15 mM $MgCl_2$, and 135 mM KCl, pH 7.5.

P-8/4x Ribozyme. The large subunit rRNA group I intron from *P. carinii* was engineered into a ribozyme to allow separate study of binding of exon mimics and catalytic activity. With saturating concentrations of 3′ exon mimic r(GUGCUCU), the rate of the exon ligation reaction is relatively fast, 10 times faster than the complete self-splicing reaction (0.9 vs 0.09 min^{-1}). The exon ligation reaction is also very precise; a single radiolabeled species is produced. A maximum of 80% of the bound 5′ exon mimic is converted into product, which suggests that most of the ribozyme folds correctly under the conditions used, and roughly 20% of the ribozyme binds 5′ exon mimic tightly but does not catalyze the reaction. It is likely that there is a subpopulation of improperly folded ribozymes that do not have the ability to catalyze the reaction. This is commonly seen with ribozymes and pre-rRNA transcripts (Bevilacqua & Turner, 1991; Lin et al., 1992; Emerick & Woodson, 1993; Uhlenbeck, 1995) and reflects our incomplete knowledge regarding reaction conditions *in vivo* and factors affecting ribozyme folding.

The 3′ Exon Mimics rGrUdGrCrUrCrU and d(GTGCTCT) Bind to P-8/4x with K_ds ≥ 40 μM. The 3′ exon mimics are expected to bind to the ribozyme by forming both P9.0 and P10 conserved helixes (Figure 1). The K_m for the reactivity of r(GUGCUCU) is 21 μM, and the K_I values, which are equivalent to K_d values, for rGrU*dG*rCrUrCrU and d(GTGCTCT) are 40 μM and 107 μM, respectively. These values can be compared with the predicted K_d of 250 μM for the r(5′GUCUCU3′)·(3′UAGAG5′) duplex (Serra & Turner, 1995), which contains the same base pairs as the P9.0 and P10 pairings. Thus, no large net stabilization of binding is evident due to the ribozyme. This may, however, reflect a combination of favorable and unfavorable interactions, since unfavorable tertiary interactions with 3′ exon mimics have been detected with the *Tetrahymena* ribozyme (Moran et al., 1993).

P-8/4x Binds the 5′ Exon Mimic r(AUGACU) with Base-Pairing and Tertiary Interactions. The stability of base pairing was estimated through thermal denaturation of the r(AUGACU)·r(GGUCAU) duplex (Table 2) and the total stability for binding to the ribozyme was obtained through band-shift gel electrophoresis (Table 1). As shown in Table 1, the stability contribution from tertiary interactions, esti-

mated to be the difference between the ΔG°_{37} for binding to the ribozyme and to r(GGUCAU), is greater than that due to formation of base pairs (6.8 kcal/mol versus 5.0 kcal/mol). Tertiary interactions decrease the K_d of r(AUGACU) binding to P-8/4x from 318 μM in the base-paired state to 5.2 nM in the catalytic complex, a factor of more than 60 000-fold. This is greater than the effect seen for 5′ exon mimics of the *Tetrahymena* ribozyme at 15 °C (4400-fold in 50 mM $MgCl_2$ and 2000-fold in 5 mM $MgCl_2$ in Hepes buffer) (Bevilacqua & Turner, 1991; Li et al., 1995) and 42 °C (6300-fold in 10 mM $MgCl_2$ in Tris buffer) (Pyle et al., 1994). The difference in tertiary stabilization could be due to differences in reaction conditions, ribozyme structure, and/or the 5′ exon mimic sequence. It is unlikely that the stability difference is due to the dangling G on the 5′ end of the P1 helix of the P-8/4x ribozyme, which is missing in the *Tetrahymena* L-21 *Sca*I ribozyme, because the increase in stability of base pairing due to 5′ dangling ends is typically less than 2-fold (0.3 kcal/mol) (Serra & Turner, 1995). It is thought that the 3′ dangling end on the P1 helix does not stack on P1 (Michel & Westhof, 1990). If it did stack, the stability increment for the *P. carinii* sequence is typically about 0.4 kcal/mol less favorable than the corresponding 3′ dangling end in *Tetrahymena* (Serra & Turner, 1995). After correction for this, the tertiary stability difference between the ribozymes would be even larger than calculated above.

The high degree of tertiary stabilization is probably important for splicing since it retains the 5′ exon intermediate in the catalytic site while the 3′ exon is brought into place for subsequent reaction (Bevilacqua et al., 1994). If these interactions can be exploited by antisense oligonucleotides, and ribosomal maturation can be inhibited, the 5′ exon binding site would be a useful target for pharmacological intervention.

The 2′ OH Groups of the 5′ Exon Mimic r(AUGACU) Do Not Make a Major Contribution to Tertiary Stabilization with the P-8/4x Ribozyme in H15Mg Buffer. To determine whether the 2′ OH groups from the 5′ exon mimic r(AUGACU) are participating in specific tertiary interactions with P-8/4x, binding was measured with 2′ OH groups of the 5′ exon mimic modified, individually and *in toto*, to 2′ H. The results show that individual 2′ OH groups can be replaced with H without decreasing stabilizing tertiary contacts with the catalytic core of P-8/4x (Table 1). This is surprising because, in both Hepes and Tris buffers, the 2′ OH groups at nucleotides −3 and −2 of the 5′ exon mimic of the *Tetrahymena* L-21 *Sca*I ribozyme each provide roughly 1 kcal/mol in tertiary stabilization with the *Tetrahymena* ribozyme's catalytic core (Bevilacqua et al., 1991; Pyle & Cech, 1991; Strobel & Cech, 1993; Li et al., 1995). There are other tertiary interactions in the *Tetrahymena* L-21 *Sca*I system, however, that help drive the docking of the P1 helix into the catalytic core: the 2′ OH groups at positions 22 and 23 of the IGS (Strobel & Cech, 1993), the exocyclic NH_2 group of G22 (Strobel & Cech, 1995), and possibly the binding of Mg^{2+} ions (Li et al., 1995) are also involved in tertiary stabilization. Presumably, other interactions are also important for P1 helix docking into the catalytic core of the P-8/4x ribozyme.

In H15Mg buffer, the P-8/4x ribozyme binds DNA 5′ exon mimics with nearly the same amount of tertiary stabilization as the RNA exon mimic (Table 1). The mimic d(ATGACT) binds more tightly than d(AUGACU). Therefore, the addition of the methyl groups does not inhibit binding of the 5′ exon mimic to the ribozyme. The CD spectra in Figure 6 suggest that RNA·RNA and RNA·DNA P1 helixes are both basically A-form, although not identical. Evidently, the difference in helix conformation is small enough for the hybrid to still maintain most of the tertiary stabilization that binds the all-RNA helix.

The P-8/4x ribozyme in H15Mg buffer binds deoxynucleotide versions of its 5′ exon mimic tightly through base-pairing and tertiary interactions, but the L-21 *Sca*I ribozyme does not. This suggests that some aspects of the tertiary interactions in the two ribozymes are different. Specifically, there are no discernable tertiary interactions in the P-8/4x ribozyme that involve 2′OH groups from the 5′ exon mimic, while there are for the L-21 *Sca*I ribozyme. The total tertiary stabilization is greater for the P-8/4x ribozyme than for the L-21 *Sca*I ribozyme, indicating that the presence or absence of the 2′OH interactions is not the only difference in tertiary interactions between the two systems. The tight binding of deoxynucleotide 5′ exon mimics to the P-8/4x ribozyme in H15Mg buffer is lost in T10Mg buffer, indicating that T10Mg buffer does not permit the tertiary interactions that are responsible for the tight binding in H15Mg. Unfortunately, the reaction conditions in the nucleus of *P. carinii* are currently unknown, so the stability of binding *in vivo* cannot be predicted.

In H15Mg buffer, substitution of any single 2′ OH group with a 2′ H in the 5′ exon mimic results in an increase or no change in the tertiary stabilization with P-8/4x (Table 1). For each substitution, however, a decrease in base-pairing stability is observed. For example, rArU*d*GrArCrU base pairs to the 5′ IGS oligonucleotide r(GGUCAU) 4 times less tightly than the unmodified mimic, while the tertiary stabilization of the variant is about 3 times that of the unmodified mimic (Table 1). Apparently, there are compensating effects between the tertiary stability and the base-pairing stability such that the overall stability is not dramatically changed. For the purposes of antisense development, this is encouraging because chemically modified oligonucleotides that result in a decrease in base-pairing stability might still be stabilized by tertiary interactions, thus providing both tight binding and specificity, as well as chemical stability.

Thermodynamics of Base Pairing. As shown in Table 2, the ΔG°_{37} of the duplex formed by r(AUGACU) and r(GGUCAU) is only about 0.6 kcal/mol different from that predicted on the basis of nearest-neighbor parameters (Serra & Turner, 1995). Thus, this duplex is not unusual in its stability. Each deoxynucleotide substitution decreases duplex stability. Generally, DNA/RNA hybrids are less stable than their RNA/RNA counterparts (Sugimoto et al., 1995). Moreover, the combination of deoxynucleotide purines base-pairing with ribonucleotide pyrimidines is the most destabilizing form of hybrid (Roberts & Crothers, 1992; Hung et al., 1994; Sugimoto et al., 1995; Gyi et al., 1996). Although every single 2′ OH to 2′ H substitution tested here results in a loss of duplex stability, greater destabilization is seen for substitution at the internal purines. The all-deoxyribonucleotide mimics form very destabilized duplexes with r(GGUCAU), as predicted (Sugimoto et al., 1995). There is no significant difference between the stability of the duplex formed with thymidine and deoxyuridine, indicating a small role or no role for the methyl group of thymidine in stabilizing this duplex.

Implications for Antisense Development. The *P. carinii* large subunit ribosomal RNA group I intron is a good model

for studying antisense targeting to structured RNAs. The group I intron and the P-8/4x ribozyme can fold and catalyze their reactions *in vitro*, therefore allowing simulation of *in vivo* group I intron behavior. The self-splicing intron provides a model for testing antisense inhibition of activity. At 37 °C, the P-8/4x ribozyme binds short 5′ exon mimics more than 60 000 times tighter than expected for base-pairing with the IGS. This binding enhancement by tertiary interactions is dependent on the three-dimensional folding of more than 100 nucleotides in the target. Thus, these mimics are rationally designed lead antisense agents that bind with considerably more specificity than possible with longer antisense agents that simply base-pair with their target. This model system also has potential medical importance. Antisense inhibition of group I intron activity would result in the disruption of ribosomal maturation of the fungi and perhaps inhibit fungal proliferation. A mouse model is convenient for testing and the mouse-derived *P. carinii* intron contains the same P1 sequence, and hence the same molecular target, as the human-derived *P. carinii* intron (Liu & Leibowitz, 1993).

It is important to remember that the P-8/4x ribozyme construct has been engineered such that the IGS is free to bind exogenous 5′ exon mimics. In the ribosomal precursor, the corresponding endogenous 5′ exon region is physically situated adjacent to its binding site on the intron, the IGS. Therefore, an exogenous mimic has to compete for binding to the IGS with the endogenous exon. The bimolecular binding reaction is at a considerable disadvantage over the intramolecular reaction. Woodson and Cech (1991) have shown that in some group I intron systems, however, the endogenous 5′ exon region that pairs with the IGS can also base-pair with an upstream 5′ exon sequence, thus freeing up the IGS for binding by an exogenous 5′ exon mimic. Secondary structure prediction by thermodynamic methods indicate that the 5′ exon of the *P. carinii* large subunit group I intron can also form such a competing structure (data not shown). In fact, exogenous 5′ exon mimics can bind and inhibit the self-splicing reaction at concentrations low enough to indicate that the IGS is at least partly accessible (S. Testa, S. Gryaznov, and D. H. Turner, unpublished experiments). In general, however, it is expected that this strategy would be most effective if the tertiary interactions being exploited for antisense targeting were in *trans* rather than *cis*, thereby eliminating the problem of having to outcompete an intramolecular binding reaction with a bimolecular reaction.

Antisense oligonucleotides that target the tertiary structure of RNAs by binding through both base-pairing and tertiary interactions can be shorter than antisense agents that only base-pair with their target RNA (Bevilacqua & Turner, 1991). This is important because long oligomers can bind tightly to sequences with mismatches, thus reducing specificity for targeting, as illustrated in Figure 7 (Herschlag, 1991; Roberts & Crothers, 1991; Woolf et al., 1992). For the case presented here, a hexamer, which at 1 μM does not form a stable helix with its complement at 37 °C, is bound in the catalytic core of the *P. carinii* large subunit rRNA group I ribozyme with a dissociation constant of about 5 nM. As illustrated in Figure 7, this represents the ultimate in specificity; the antisense, at a concentration of 1 μM, binds all its intended target and nothing else. Other advantages to using short antisense oligonucleotides include cheaper and easier production (Wagner et al., 1996) and potentially more facile transfer across membranes (Loke et al., 1989).

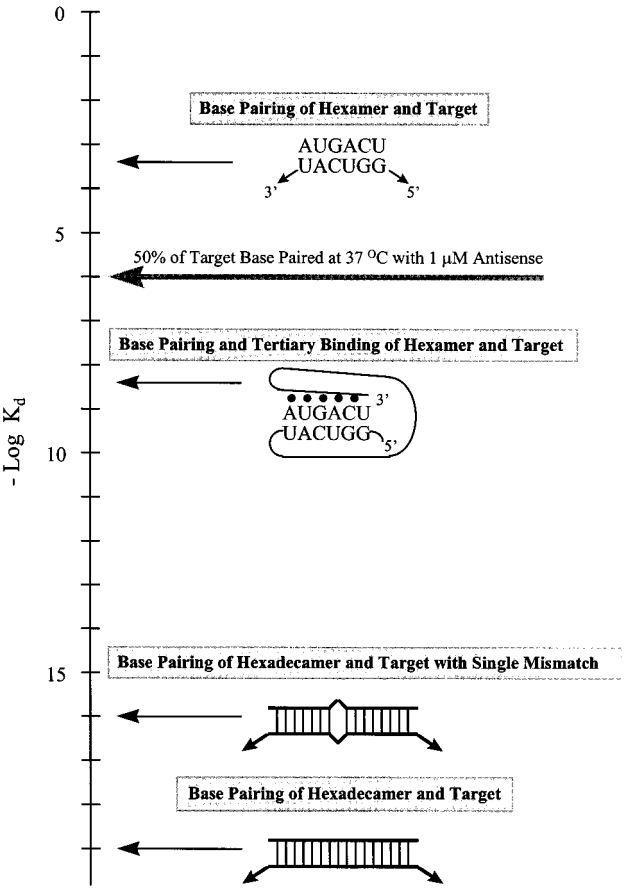

FIGURE 7: Sequence recognition of RNA targets by base-pairing and tertiary interactions when antisense is in excess of target. The dissociation constant, K_d, of a hexadecamer forming a perfectly matched or even a mismatched helix can be extremely small. Thus, both matched and mismatched targets may be completely bound in the presence of 1 μM antisense agent (Herschlag, 1991; Roberts & Crothers, 1991; Woolf et al., 1992). This is problematic since long oligonucleotides are required to target a single sequence from the human genome but may not discriminate against sequences containing a single mismatch. The K_d of r(AUGACU) base pairing with its complement at 37 °C is about 300 μM. Therefore, this hexamer at 1 μM will not stably base-pair with its complement at 37 °C. The K_d for binding to the RNA target by base-pairing and tertiary interactions, however, is about 5 nM (Table 1). Thus target will be completely bound at 1 μM r(AUGACU), and because r(AUGACU) will not stably base-pair with any sequence, the binding is very specific. Specificity is further increased in this example because the group I intron tertiary site being targeted is not present in humans. For the hexadecamer helixes, $\Delta G°_{37}$ is approximated as the sum of the $\Delta G°_{37}$ values for helix initiation (about 3 kcal/mol) and base pairing (about 2 kcal/mol per nearest neighbor interaction) and the penalty for single mismatch formation (about 1 kcal/mol) (Serra & Turner, 1995).

In H15Mg buffer, the P-8/4x ribozyme binds DNA 5′ exon mimics nearly as tightly as RNA mimics. This shows, for the first time, that DNA oligonucleotides can bind to a structured RNA by exploiting tertiary interactions. DNA and related analogues without a 2′ OH are cheaper and easier to produce and are chemically more stable than RNA, which are advantages for antisense applications. Thus, the *P. carinii* large subunit rRNA group I intron is a good system for studying the factors affecting recognition of antisense compounds by tertiary interactions.

SUMMARY AND CONCLUSIONS

We have cloned and characterized a group I intron embedded within the large subunit ribosomal RNA from the

fungal pathogen *Pneumocystis carinii*. Because the group I intron is embedded in ribosomal RNA, it is likely that disruption of the autoexcision process of the intron will disrupt ribosomal maturation, ultimately affecting fungal proliferation. The self-splicing intron was engineered into a ribozyme, which is catalytically active. Due to tertiary interactions, the exogenous 5′ exon mimic r(AUGACU) binds to the ribozyme about 60 000 times more tightly than expected for base-pairing. In a buffer containing 50 mM Hepes (25 mM Na^+), 15 mM $MgCl_2$, and 135 mM KCl at pH 7.5, the 2′ OH groups on the 5′ exons are not required for this tertiary stabilization. Thus small oligonucleotides lacking 2′ OH groups can exploit the tertiary interactions inherent in functional RNAs. These results suggest a new paradigm for antisense targeting in which binding enhancement by tertiary interactions (BETI) provides a dramatic increase in specificity of targeting.

REFERENCES

Barfod, E. T., & Cech, T. R. (1989) *Mol. Cell. Biol. 9*, 3657−3666.

Baserga. R., & Denhardt, D. T., Ed. (1992) *Antisense Strategies*; Annals of the New York Academy of Sciences, Vol. 660, New York Academy of Sciences: New York.

Bass, B. L., & Cech, T. R. (1984) *Nature 308*, 820−826.

Bevilacqua, P. C., & Turner, D. H. (1991) *Biochemistry 30*, 10632−10640.

Bevilacqua, P. C., Kierzek, R., Johnson, K. A., & Turner, D. H. (1992) *Science 258*, 1355−1358.

Bevilacqua, P. C., Li, Y., & Turner, D. H. (1994) *Biochemistry 33*, 11340−11348.

Bevilacqua, P. C., Sugimoto, N., & Turner, D. H (1996) *Biochemistry 35*, 648−658.

Borer, P. N., Dengler, B., Tinoco, I., Jr., & Uhlenbeck, O. C. (1974) *J. Mol. Biol. 86*, 843−853.

Cech, T. R., Zaug, A. J., & Grabowski, P. J. (1981) *Cell 27*, 487−496.

Chrissey, L. (1991) *Antisense Res. Dev. 1*, 65−113.

Damberger, S. H., & Gutell, R. R. (1994) *Nucleic Acids Res.* 3508−3510.

Davanloo, P., Rosenberg, A. H., Dunn, J. J., & Studier, F. W. (1984) *Proc. Natl. Acad. Sci. U.S.A. 81*, 2035−2039.

Emerick, V. L., & Woodson, S. A. (1993) *Biochemistry 32*, 14062−14067.

Fersht, A. (1985) *Enzyme Structure and Mechanism*, 2nd ed., W. H. Freeman and Company, New York.

Freier, S. M., Kierzek, R., Jaeger, J. A., Sugimoto, N., Caruthers, M. H., Neilson, T., & Turner, D. H. (1986) *Proc. Natl. Acad. Sci. U.S.A. 83*, 9373−9377.

Fried, M., & Crothers, D. M. (1981) *Nucleic Acids Res. 9*, 6505−6525.

Garner, M. M., & Revzin, A. (1981) *Nucleic Acids Res. 9*, 3047−3060.

Gyi, J. I., Conn, L. G., Lane, A. N., & Brown, T. (1996) *Biochemistry 35*, 12538−12548.

Harrison, P. M., & Hoare, R. J. (1980) in *Metals in Biochemistry*, pp 7−13, Chapman and Hall Ltd., New York.

Herschlag, D. (1991) *Proc. Natl. Acad. Sci. U.S.A. 88*, 6921−6925.

Herschlag, D. (1992) *Biochemistry 31*, 1386−1399.

Herschlag, D., Eckstein, F., & Cech, T. R. (1993) *Biochemistry 32*, 8299−8311.

Hung, S.-H., Tu, Q., Gray, D. M., & Ratliff, R. L. (1994) *Nucleic Acids Res. 22*, 4326−4334.

Letsinger, R. L., & Lunsford, W. B. (1975) *J. Am. Chem. Soc. 98*, 3655−3661.

Li, Y., Bevilacqua, P. C., Matthews, D., & Turner, D. H. (1995) *Biochemistry 34*, 14394−14399.

Lin, S.-Y., & Riggs, A. D. (1972) *J. Mol. Biol. 72*, 671−690.

Lin, H., Niu, M. T., Yoganathan, T., & Buck, G. A. (1992) *Gene 119*, 163−173.

Liu, Y., & Leibowitz, M. J. (1993) *Nucleic Acids Res. 21*, 2415−2421.

Liu, Y., Rocourt, M., Pan, S., Liu, C., & Leibowitz, M. J. (1992) *Nucleic Acids Res. 20*, 3763−3772.

Loke, S. L., Stein, C. A., Zhang, X. H., Mori, K., Nakanishi, M., Subasinghe, C., Cohen, J. S., & Neckers, L. M. (1989) *Proc. Natl. Acad. Sci. U.S.A. 86*, 3474−3478.

Longfellow, C. E., Kierzek, R., & Turner, D. H. (1990) *Biochemistry 29*, 278−285.

Matteucci, M. D., & Caruthers, M. H. (1980) *Tetrahedron Lett. 21*, 719−722.

McDowell, J. A., & Turner D. H. (1996) *Biochemistry 35*, 14077−14089.

Michel, F., & Westhof, E. (1990) *J. Mol. Biol. 216*, 585−610.

Moran, S., Kierzek, R., & Turner, D. H. (1993) *Biochemistry 32*, 5247−5266.

Nikolcheva, T., & Woodson, S. A. (1997) *RNA 3*, 1016−1027.

Puglisi, J. D., & Tinoco, I., Jr. (1989) *Methods Enzymol. 180*, 304−325.

Pyle, A. M., & Cech, T. R. (1991) *Nature 350*, 628−631.

Pyle, A. M., McSwiggen, J. A., & Cech, T. R. (1990) *Proc. Natl. Acad. Sci. U.S.A. 87*, 8187−8191.

Pyle, A. M., Murphy, F. L., & Cech, T. R. (1992) *Nature 358*, 123−128.

Pyle, A. M., Moran, S., Strobel, S. A., Chapman, T., Turner, D. H., & Cech, T. R. (1994) *Biochemistry 33*, 13856−13863.

Roberts, R. W., & Crothers, D. M. (1991) *Proc. Natl. Acad. Sci. U.S.A. 88*, 9397−9401.

Roberts, R. W., & Crothers, D. M. (1992) *Science 258*, 1463−1466.

Sambrook, J., Fritsch, E. F., & Maniatis, T. (1989) *Molecular Cloning: A Laboratory Manual*, *Second Edition*. Cold Spring Harbor Laboratory Press, Cold Spring Harbor, NY.

SantaLucia, J., Jr., Kierzek, R., & Turner, D. H. (1991a) *J. Am. Chem. Soc. 113*, 4313−4322.

SantaLucia, J., Jr., Kierzek, R., & Turner, D. H. (1991b) *Biochemistry 30*, 8242−8251.

Serra, M. J., & Turner, D. H. (1995) *Methods Enzymol. 259*, 242−261.

Sinha, N. D., Biernat, J., McManus, J., & Köster, H. (1984) *Nucleic Acids Res. 12*, 4539−4557.

Sternberg, S. (1994) *Science 266*, 1632−1634.

Strobel, S. A., & Cech, T. R. (1993) *Biochemistry 32*, 13593−13604.

Strobel, S. A., & Cech, T. R. (1995) *Science 267*, 675−679.

Sugimoto, N., Nakano, S., Katoh, M., Matsumura, A., Nakaamuta, H., Ohmichi, T., Yoneyama, M., & Sasaki, M. (1995) *Biochemistry 34*, 11211−11216.

Tanner, M. A., & Cech, T. R. (1996) *RNA 2*, 74−83.

Uhlenbeck, O. C. (1995) *RNA 1*, 4−6.

Usman, N., Ogilvie, K. K., Jiang, M.-Y., & Cedergren, R. J. (1987) *J. Am. Chem. Soc. 109*, 9845−9854.

Wagner, R. W., Matteucci, M. D., Grant, D., Huang, T., & Froehler, B. C. (1996) *Nat. Biotechnol. 14*, 840−844.

Wang, J.-F., Downs, W. D., & Cech, T. R. (1993) *Science 260*, 504−508.

Weeks, K. M., & Crothers, D. M. (1992) *Biochemistry 31*, 10281−10287.

Weeks, K. M., & Cech, T. R. (1995) *Biochemistry 34*, 7728−7738.

Woodson, S. A., & Cech, T. R. (1991) *Biochemistry 30*, 2042−2050.

Woolf, T. M., Melton, D. A., & Jennings, C. G. B. (1992) *Proc. Natl. Acad. Sci. U.S.A. 89*, 7305−7309.

Xia, T., McDowell, J. A., & Turner, D. H. (1997) *Biochemistry 36*, 12486−12497.

Zaug, A. J., Grosshans, C. A., & Cech, T. R. (1988) *Biochemistry 27*, 8924−8931.

Zaug, A. J., McEvoy, M. M., & Cech, T. R. (1993) *Biochemistry 32*, 7946−7953.

BI9713097